

Synthesis, Structure, and Electron Density Distribution in Crystals of $K_2(L\text{-Trp})_2(H_2O)$ (HTrp = Tryptophane)

N. A. Bondareva^a, P. P. Purygin^a, Yu. P. Zarubin^a, P. V. Dorovatovskii^b,
A. A. Korlyukov^{c, d}, and A. V. Vologzhanina^{d, *}

^a Samara National Research University, Samara, Russia

^b National Research Center Kurchatov Institute, Moscow, Russia

^c Pirogov Russian National Research Medical University, Moscow, Russia

^d Nesmeyanov Institute of Organoelement Compounds, Russian Academy of Sciences, Moscow, Russia

*e-mail: vologzhanina@mail.ru

Received July 18, 2022; revised August 21, 2022; accepted August 23, 2022

Abstract—The first salt of alkaline metal and L-tryptophane, $K_2(L\text{-Trp})_2(H_2O)$ (I), is synthesized by the reaction of L-tryptophane (HTrp) with potassium hydroxide in an aqueous-alcohol solution. Compound I is characterized by IR and 1H NMR spectroscopy and X-ray diffraction (XRD) (CIF file CCDC no. 2184367). Compound I is found to have a layered structure due to the presence of the bridging water molecule and chelate-bridging anions. The quantum chemical calculations of the crystal structure (PBE, plane-wave basis set, 800 eV) is used to evaluate the strength of interactions of the potassium ion with the L-tryptophanate anion (depending on the coordination type) and the influence of the anion conformation on the strength of coordination, hydrophobic, and hydrophilic interactions.

Keywords: L-tryptophane, potassium salts, periodic quantum chemical calculations, crystal structure, Voronoi–Dirichlet polyhedra

DOI: 10.1134/S1070328423700483

INTRODUCTION

The study of interactions of metal complexes with biomacromolecules, for instance, DNA and proteins, is an important trend of investigations in biochemistry, medical chemistry, and pharmacy [1–4]. The purposes of the studies are both the reaction routes of these interactions and the energy of the interactions and possible changes in the coordination sphere of metal atoms. The most part of studies of this type is performed using DFT calculations of metalloproteins or complexes of macromolecules with small metal-containing molecules [5]. However, model systems showing the interactions of the metal cation with individual amino acid residues or small proteins can also provide a valuable information about specific features of the coordination mode and nature of metal–amino acid interactions [4, 6].

We were interested in tryptophane complexes, since Trp is one of essential amino acids having simultaneously (due to the indole ring) the largest hydrophobic surface and the additional hydrogen bond donor atom N^1 (NH group) [7, 8]. To date, 36 compounds containing D-, L-, or DL-amino acid have structurally been characterized, and only four of them ($[Cu(L\text{-Trp})_2]$ [9], $[Fe(DL\text{-Trp})_2]$ [10], $[Ni(DL\text{-Trp})_2]$ [11], and $[Mn(DL\text{-Trp})_2]$ [12]) contain no other ligands, except for Trp and solvent molecules. All compounds based on enantiomerically pure amino acids crystallize in noncentrosymmetric space groups, which makes it possible to use them as nonlinear optical materials [13]. Some of the synthesized compounds manifest a slow magnetic relaxation [14], selectively sorb selected amino acids [15], or induce DNA helix cleavage [16, 17]. Potassium is one of the most abundant biometals and a component of pharmaceutical salts. Potassium atoms are observed only in one of the earlier studied compounds: $K[Co^{III}(Bcmpa)(Trp)] \cdot 2H_2O$ (Bcmpa $^{3-}$ is N,N -bis(carboxymethyl)-(S)-phenyl alaninate) [18].

The purpose of this work is to synthesize potassium L-tryptophanate and study its structure and specific features of amino acid coordination by the alkaline metal.

EXPERIMENTAL

Commercial (Sigma–Aldrich) potassium hydroxide (KOH) and L-tryptophane (HTrp) were used as received. IR spectra were recorded on a Bruker Tensor-27 spectrometer using KBr. The NMR spectrum (1H , 400 MHz) was measured on a Bruker Advance II

instrument in DMSO-d₆ using TMS as the external standard. The melting point was determined with a Stuart SMP10 instrument.

Synthesis of catena((μ₃-L-tryptophanato-O,O',O',N)(μ₅-L-tryptophanato-O,O,O',O',O')(μ₃-aqua)dipotassium) [K₂(μ₃-L-Trp-O,O',N)(μ₅-L-Trp-O,O')(μ₃-H₂O)]_n (I). Potassium hydroxide (2.80 g, 0.050 mol) was added by portions to a suspension of tryptophane (5.10 g, 0.025 mol) in water (20 mL). The reaction mixture was heated at 95°C for 40 min. The homogeneous solution was evaporated and dried at room temperature. The formed crystals were filtered off. The yield of compound I was 6.00 g (80%). Salt I is a highly melting product, highly soluble in water, and insoluble in alcohol and acetone. The crystals of compound I suitable for XRD were grown from an aqueous-alcohol mixture.

IR (KBr; ν , cm⁻¹): 3051–3090 ν (N–H), 1720–1755 ν _{as}(C=O), 1416 ν _{as}(CH₃). ¹H NMR (DMSO-d₆; 400 MHz; δ , ppm): 3.03 m (NH₂), 3.26 d, 3.43 m (α -CH), 7.23 m (H⁵, H⁶ Ind, 2H), 7.35 dd (CH), 7.41 d (H⁴ Ind, 1H), 7.60 d (H⁷ Ind, H), 8.39 s (NH).

XRD was carried out on the K4.4 Belok/XSA diffraction beamline of the National Research Center Kurchatov Institute (Moscow, Russia) at 100.0(2) K [19, 20] using a MarDTB 1-axial goniometer equipped with a Rayonix SX165 CCD 2D detector (λ = 0.745 Å, φ scan mode with an increment of 1.0°, direct geometry) mounted perpendicularly to the radiation source. The crystals of C₁₁H₁₂KN₂O_{2.5} (*FW* = 251.33) are monoclinic (space group *P*2₁): a = 8.3750(17), b = 6.3340(13), c = 21.807(4) Å, β = 99.75(3)°, V = 1140.1(4) Å³, Z = 4, ρ = 1.464 g cm⁻³, μ = 0.517 mm⁻¹. Absorption corrections were applied to the experimentally determined reflection intensities, which were obtained in the XDS software [21], using the Scala program [22].

The structure was solved by the conjugate space method implemented in the SHELXT software [23] and refined by full-matrix least squares for F^2 using SHELXL-2014 [24] for all data in the anisotropic approximation for all non-hydrogen atoms using the Olex2 program [25]. Hydrogen atoms were placed in geometrically calculated positions and refined by the riding model with isotropic thermal parameters equal to $U_{\text{iso}} = 1.5U_{\text{eq}}(\text{O})$ for water molecules and $U_{\text{iso}} = 1.2U_{\text{eq}}(\text{X})$ for other atoms, where $U_{\text{eq}}(\text{X})$ are equivalent isotropic thermal parameters of the atom to which the hydrogen atom is bound. The structure factors were $R_1 = 0.0362$ (for 5740 observed reflections and $wR_2 = 0.0954$ (for 6199 independent reflections, $R_{\text{int}} = 0.0390$, GOOF = 1.060).

The additional crystallographic information for the structure of compound I was deposited with the Cambridge Crystallographic Data Centre (CIF file CCDC no. 2184367; <http://www.ccdc.cam.ac.uk/structures>).

A comparative analysis of nonvalence interactions in tryptophanates of different metals was performed using the Voronoi–Dirichlet molecular polyhedra [26, 27] in the ToposPro software [28].

Quantum chemical study of the crystal structure of compound I was carried out using the VASP 5.4.1 software [29–33] with the optimization of atomic coordinates. The plane-wave basis set with a maximum kinetic energy of 800 eV was used for the description of valence electrons. The exchange and correlation contributions to the total energy were calculated using the PBE functional. The PAW potentials with a minimum possible sphere radius described by the pseudo-wave function (“hard PAW potentials”) were used for geometry optimization and subsequent calculation of the electron density function. The optimization criterion was the maximum force magnitude equal to 0.01 eV/Å².

The electron density function for topological analysis was obtained by the particular calculation of the optimized crystal structure. The AIM program (a part of the ABINIT software [34]) was used for topological analysis of the theoretical electron density distribution function $\rho(\mathbf{r})$. Atomic charges were calculated using the Bader program [35].

RESULTS AND DISCUSSION

The reaction of L-tryptophane and potassium hydroxide in an aqueous solution on heating afforded a white precipitate soluble in water and insoluble in alcohol and acetone. Since the structure of potassium tryptophanate dihydrate contains water molecules, the stretching vibrations of the OH groups are overlapped with the stretching vibrations of the carboxylate group to form a total broad absorption band in a range of 1720–1755 $\nu_{\text{as}}(\text{C=O})$, which does not allow a precise assignment of the corresponding stretching vibration frequencies. The molecular and crystal structures of compound I were determined by XRD. Compound I crystallizes in the noncentrosymmetric space group *P*2₁ with two cations, two anions, and one water molecule in the independent part of the unit cell (Fig. 1). In the difference synthesis, the hydrogen atoms are on the carbon atoms, on the nitrogen atoms of the heterocycle and amino group, and on the oxygen atom of the water molecule, which makes it possible to unambiguously establish the deprotonation of HTrp at the carboxy group. The presence of two independent cations and anions can be considered as caused by different types of the coordination environment of the ions in the structure of compound I. The cations form coor-

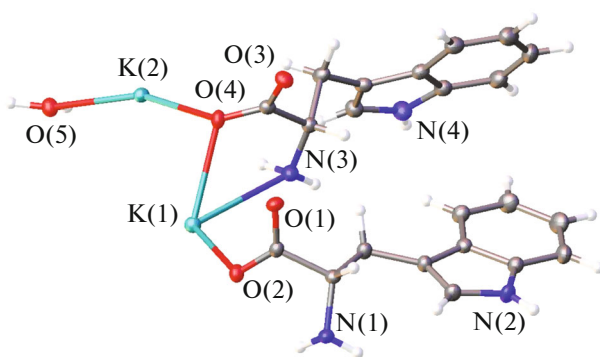


Fig. 1. Independent part of the unit cell in the structure of compound **I** in the representation of atoms by thermal ellipsoids ($p = 50\%$).

dination polyhedra $\text{K}(1)\text{NO}_6$ and $\text{K}(2)\text{O}_8$ (Fig. 2) in which the $\text{K}(1)-\text{N}(3)$ bond length is $2.951(2)$ Å and the $\text{K}-\text{O}$ bond lengths range from $2.590(2)$ to $3.046(2)$ Å (Table 1).

The coordination sphere of the $\text{K}(1)$ atom is formed by the water molecule and four anions, two of which are coordinated via one oxygen atom of the carboxy group, one atom is coordinated via the two oxygen atoms of the carboxy group, and one more atom is coordinated via the oxygen atom of the carboxy group and nitrogen atom of the amino group with the formation of the five-membered ring. The $\text{K}(2)$ cation is linked with two water molecules, four anions (via one oxygen atom of the carboxy group), and one anion (via both atoms of the carboxy group) to form a four-membered ring. One of the anions is bridging-chelate and is bound to three cations due to the amino and carboxy groups. The second anion chelates one cation and is additionally linked with four cations. The coordination modes of the tryptophanate anions in compound **I** and in the previously studied metal tryptophanates are schematically shown in Scheme 1. As can be seen from the data presented, both coordination modes are new for this ligand and for the first time show a possibility of coordination to the metal atom without amino group participation.

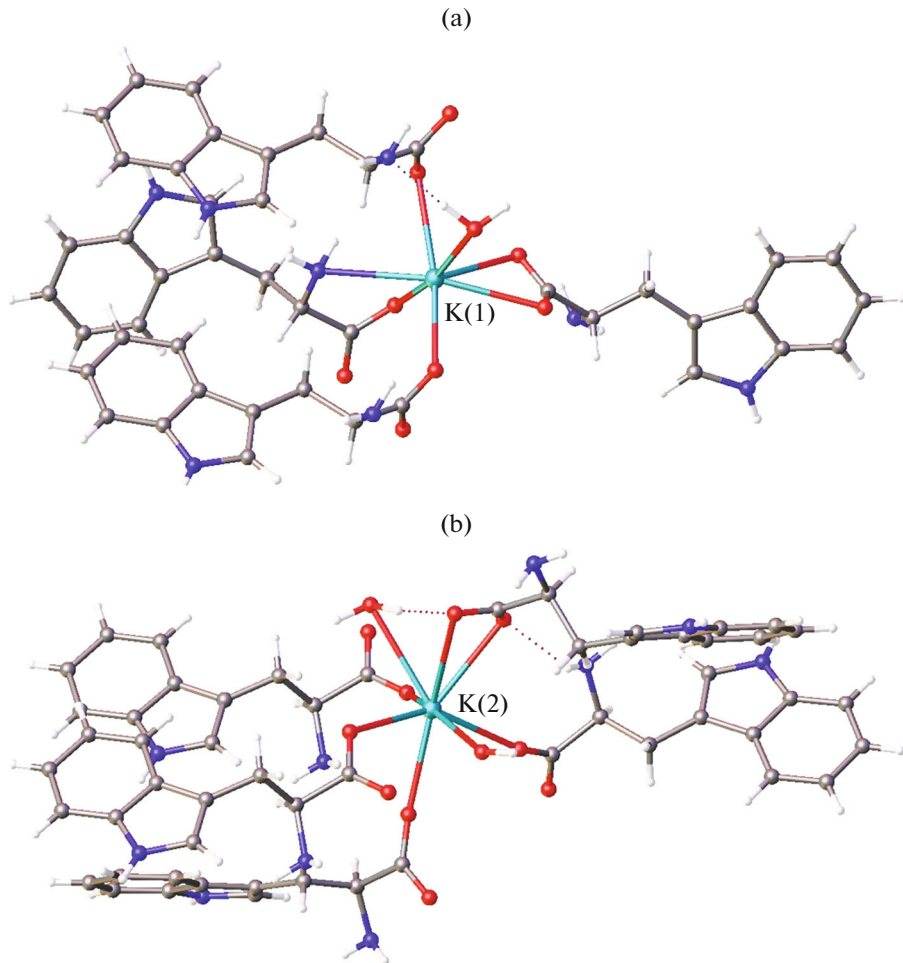


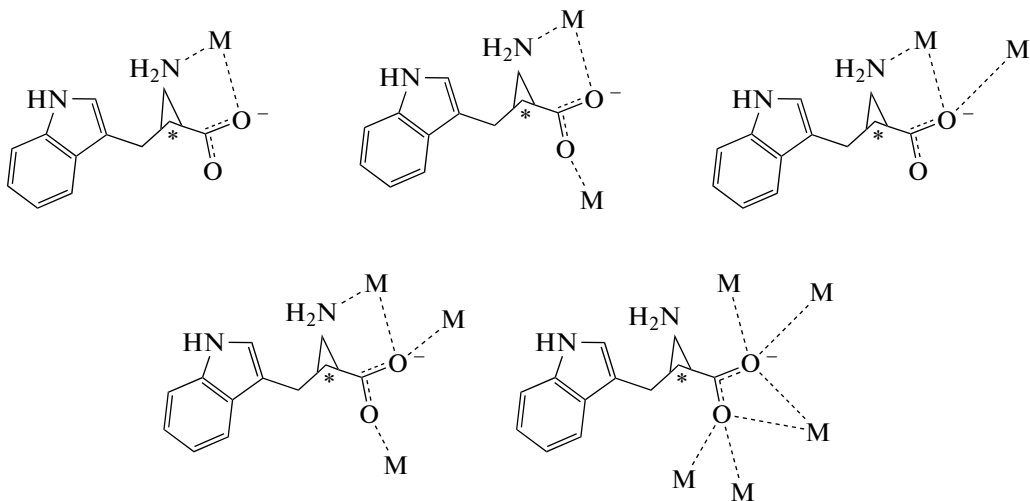
Fig. 2. Coordination environment of the (a) $\text{K}(1)$ and (b) $\text{K}(2)$ atoms in the structure of compound **I**.

Table 1. Characteristics of coordination spheres of potassium atoms in the structure of compound I*

Bond	d_{exp} , Å	d_{theor} , Å	Ω , %	$\rho(\mathbf{r})$, a.u.	$\nabla^2\rho(\mathbf{r})$, a.u.	$V(\mathbf{r})$, a.u.	E_b , kcal mol ⁻¹
K(1)–O(1) ⁱ	2.800(2)	2.819	9.6	0.0179	0.0803	-0.014	-4.30
K(1)–O(1) ⁱⁱ	2.737(2)	2.755	9.9	0.0221	0.0986	-0.018	-5.71
K(1)–O(2)	2.590(2)	2.601	16.7	0.0305	0.1372	-0.029	-8.95
K(1)–O(2) ⁱ	2.804(2)	2.838	9.6	0.0189	0.0846	-0.015	-4.63
K(1)–O(4)	2.680(2)	2.694	11.6	0.0250	0.1123	-0.022	-6.77
K(1)–O(5) ⁱⁱⁱ	2.814(2)	2.866	11.0	0.0202	0.0875	-0.016	-4.98
K(1)–N(3)	2.951(2)	2.976	5.1	0.0157	0.0633	-0.011	-3.43
K(1)–H(2A) ⁱⁱ	2.834	2.779	9.6	0.0082	0.0362	-0.005	-1.55
K(2)–O(1) ⁱⁱ	2.738(2)	2.755	12.0	0.0195	0.0974	-0.016	-5.09
K(2)–O(2) ⁱ	2.846(2)	2.872	11.0	0.0147	0.0751	-0.011	-3.54
K(2)–O(3) ⁱⁱ	2.843(2)	2.866	11.4	0.0167	0.0748	-0.012	-3.91
K(2)–O(3) ^{iv}	2.870(2)	2.887	10.0	0.0165	0.0762	-0.012	-3.91
K(2)–O(4) ^{iv}	3.046(2)	3.059	4.3	0.0116	0.0516	-0.008	-2.42
K(2)–O(4)	2.696(2)	2.725	12.6	0.0222	0.1043	-0.019	-5.87
K(2)–O(5) ^v	3.020(2)	2.959	3.6	0.0147	0.0659	-0.11	-3.30
K(2)–O(5)	2.694(2)	2.705	12.6	0.0237	0.1098	-0.020	-6.39

* d_{exp} and d_{theor} are interatomic distances in the experimental structure and in the calculations performed with geometry optimization;

Ω is the solid angle of the VDP face corresponding to this distance (in % of 4π steradian); $\rho(\mathbf{r})$, $\nabla^2\rho(\mathbf{r})$, and $V(\mathbf{r})$ are the electron density, electron density Laplacian, and potential energy density at the critical bond point, respectively; and E_b is the contact energy defined as $0.5V(\mathbf{r})$. Symmetry codes: ⁱ $1-x, 1/2+y, 1-z$; ⁱⁱ $x, 1+y, z$; ⁱⁱⁱ $1-x, -1/2+y, 1-z$; ^{iv} $-x, 1/2+y, 1-z$; ^v $-x, -1/2+y, 1-z$.

**Scheme 1.**

We succeeded in unambiguously confirming the coordination modes for the ligands and in establishing the coordination environment of the metal atoms by means of periodic quantum calculations. The most part of coordination bonds elongate after geometry optimization (Table 1), but the coordination mode of the ligands determined by an analysis of $\rho(\mathbf{r})$ in terms

of R. Bader's theory "Atoms in Molecules" [36, 37] remains unchanged. The point corresponding to the agostic contact $K(1)\cdots H(2A)-C(2)$ was found for the K(1) atom along with bonding critical points corresponding to the expected bonds with the oxygen and nitrogen atoms. The formation of the bonding contact with this atom becomes possible due to the partially

negative charge on the H(2A) atom, unlike the hydrogen atoms of the amino groups and water molecules that also arranged at distances of 2.734–3.197 Å from the potassium atoms. Note that bonding interactions in the coordination sphere of the potassium atoms can be revealed using the Voronoi–Dirichlet atomic polyhedra (VDP), where a common major face for two atoms indicates an interaction [38–40]. The major faces of the VDP of the metal atoms (direct contacts with the nonzero solid angle Ω expressed in % of 4π steradian) correspond to all bonds listed in Table 1, whereas minor faces (indirect interactions and direct interactions with $\Omega < 6\%$) correspond to other forced contacts. Thus, as shown previously for the tin and cesium atoms [38, 39], direct faces of the VDP with $\Omega > 7\%$ correspond to agostic interactions.

The tryptophanate anion is structurally nonrigid because of four ordinary bonds in its structure. The experimentally observed conformations of L-Trp in the structures of the salts with conjugated atoms of the stereocenter and its environment shown in Fig. 3 indicate that the N–C–C–O torsion angle in the five-membered metallocycle varies from 8.9° to 44.4° in spite of the coordination by the metal atoms. The relatively free rotation of the heterocyclic fragment results in the formation of “contracted” and “linear” (on the whole) conformations in which the heterocycle is directed toward the coordinated metal atom or, correspondingly, from it. In the first case, the formation of metal– π interactions in which tryptophane is often involved in metal-containing biomacromolecules can be expected. In addition to the interatomic distance and value of Ω , the interaction between a pair of atoms can be characterized by the rank of face (RF) of the VDP, which shows the number of valence bonds between these atoms and changes from 0 (intermolecular contacts) and 1 (valence and coordination bonds) to infinity (intramolecular contacts). It has previously been shown for a series of compounds forming several polymorphic species that they are characterized by a unique set of faces corresponding to $RF = 0, 1, >1$ [41–43]. It was proposed to visualize specific features of molecular interactions in crystals of the polymorphs by the (RF, d) plot, where d is the interatomic distance [44].

As a rule, the conformations of the structurally nonrigid molecule are characterized by a set of torsion angles corresponding to rotation around ordinary bonds. However, this approach does not allow one to evaluate what intramolecular interactions are characteristic of this or another conformation. On the contrary, specific features of constructing atomic and molecular VDP make it possible to characterize each conformer by a set of intramolecular contacts with $RF > 1$ and visualize them on the (RF, d) plot, which can be used, for instance, for an analysis of conformations of photochromic compounds, where a particular intramolecular contact describes the initial step of the photochemical reaction [41]. The connectivity



Fig. 3. Conformations of L-Trp in the structurally characterized compounds. Hydrogen atoms are omitted. The atom of the stereocenter and three non-hydrogen atoms bound to it are superimposed.

matrix of all atoms was calculated to analyze metal– π interactions in the sampling of 23 salts containing the L-tryptophanate anion. Then the matrix was modified in such a way that all nonmetal atoms, which do not belong to the tryptophanate anions, would be considered as points, which were not bound to other atoms and, correspondingly, were involved only in interactions with $RF = 0$. The (RF, d) plot was constructed only for the interactions involving metal atoms. Hydrogen atoms were ignored, since their coordinates were determined not for all structures, calculation results can be sensitive to the N–H, O–H, and C–H bond lengths normalized or not normalized to the neutron diffraction distance, and positions of hydrogen atoms in the protein complexes are almost always unknown. The (RF, d) distribution for the copper and potassium atoms in the structures of $[\text{Cu}(\text{L-Trp})(\text{Dppa})(\text{H}_2\text{O})](\text{NO}_3)_2 \cdot \text{CH}_3\text{OH}$ (Dppa is dipyrido[3,2-*a*:2',3'-*c*]phenazine) [16] and compound I are shown in Figs. 4a and 4b, respectively. Unlike copper atoms, in the case of potassium atoms, the distribution of K–O and K–N coordination bond lengths, K...H agostic interactions, and K...K and K...C forced contacts is not discrete, because the “contracted” conformation of L-Trp in the copper complex provides a number of intramolecular contacts Cu...C ($RF = 4–6$), and the coordination number of Cu(II) equal to 5 provides an additional contact Cu...O with $RF = 0$ ($\text{Cu} \cdots \text{O}$ 3.921 Å). An analysis of (RF, d) for other compounds made it possible to reveal a series of other copper complexes with the “contracted” conformation of the tryptophanate anion, whereas in the salts of all other metal atoms the linear conformation of the

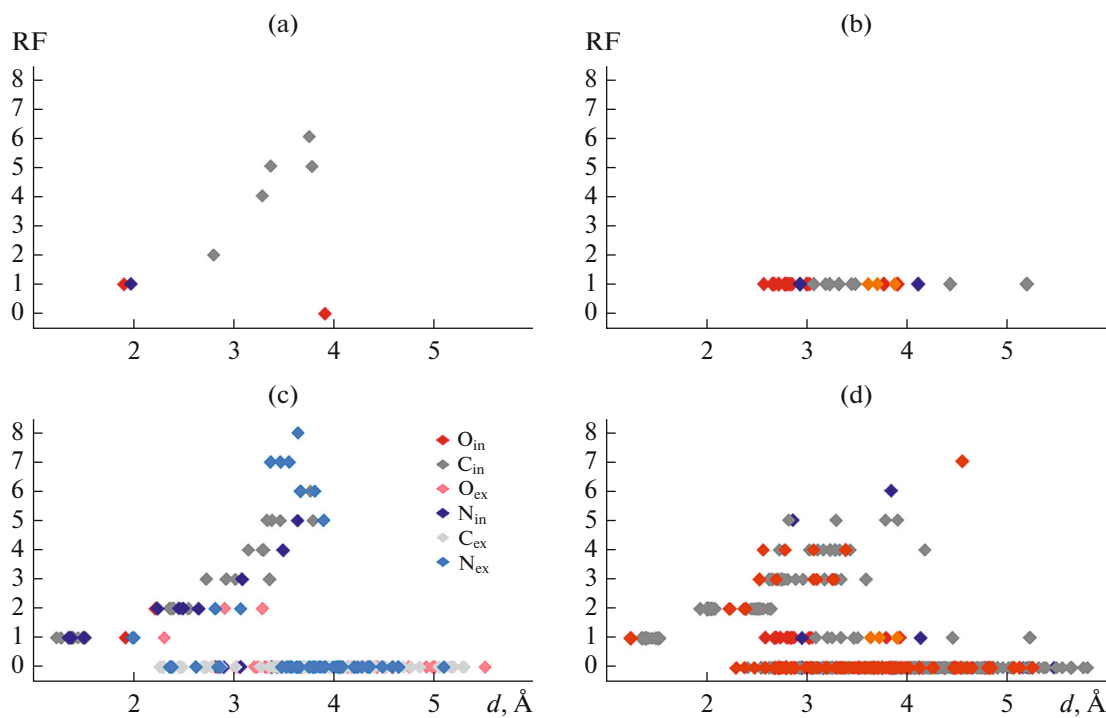


Fig. 4. Dependences (RF, d) for the Voronoi-Dirichlet polyhedra of the (a) copper atoms and (c) all atoms in the structure of $[\text{Cu}(\text{L-Trp})(\text{Dppa})(\text{H}_2\text{O})](\text{NO}_3)\cdot\text{CH}_3\text{OH}$; and (b) potassium atoms and (d) all atoms in the structure of compound I. O_{in} , C_{in} , and N_{in} are the atoms of the environment belonging to one tryptophanate anion; O_{ex} , C_{ex} , and N_{ex} are the atoms of the environment belonging to other anions and ligands in the structure of compound I.

anion and high coordination numbers result in the absence of VDP faces of the metal atom with $\text{RF} > 1$. Different conformations of the anions are shown as (RF, d) plots for all atoms of the tryptophanate anion (Figs. 4c, 4d) demonstrating the bond length distributions of all contacts found for the atoms of the anion with the assignment of the nature of the atoms of the environment. Many intramolecular interactions for both the anion itself and interactions of the anion with the Dppa atoms are observed for the “contracted” conformation of the ligand in the isolated $[\text{Cu}(\text{L-Trp})(\text{Dppa})(\text{H}_2\text{O})]^+$ complex. These contacts correspond to the stacking interactions of two heterocycles. In the case of compound I, the contacts with $\text{RF} > 1$, which are omitted in Fig. 4b, correspond to the interactions of the atoms between the adjacent anions bound by the potassium atoms rather than inside the anion itself (for the description of the layers, see below). Although the most part of contacts is formed by carbon atoms, the contacts can involve both stacking interactions and C–H \cdots π contacts, because positions of the hydrogen atoms were ignored in the calculations of the molecular VDP.

Since both tryptophane anions and also the water molecule are bridging between the potassium atoms, the whole structure of $\text{K}_2(\mu_3\text{-L-Trp-}O,O',N)(\mu_5\text{-L-Trp-}O,O')(\mu_3\text{-H}_2\text{O})$ forms infinite layers parallel to the (001) plane. Hydrogen bonds involving one of the

amino groups, the water molecule, and carboxyl residues represent an additional factor stabilizing these layers. The characteristics of these hydrogen bonds are listed in Table 2. Note that the H(N) atoms of the heterocycles and three of four atoms of the amino groups are not involved in hydrogen bond formation, because their mutual arrangement prevents this process. The layers of the bound coordination polyhedra of the cations are covered from both sides by the hydrophobic heterocyclic fragments (Fig. 5) in such a way that the H(N) atoms participate only in H \cdots H and H \cdots π contacts. An analysis in the framework of the described procedure suggests that compound I should form materials with the superhydrophobic surface. Unfortunately, a sample of compound I turned out to be contaminated with residues of the starting KOH and decomposition products of the target compound, which did not allow us to study its hydrophobic properties.

Such integral characteristics of the main structural fragments in the structure of compound I as the charge (Q), volume of the domain restricted by the zero flux surface (V_{theor}), and Voronoi-Dirichlet polyhedron volume (V_{VDP}) are given in Table 3. As can be seen from the data presented, the volume of potassium atoms is independent (at least explicitly) of the nature of the environmental atoms. The Voronoi-Dirichlet polyhedra describe the volume of structural units with

Table 2. Geometric parameters of hydrogen bonds in the structure of compound I*

D—H···A	Distance, Å			Angle DHA, deg	Ω , %	$\rho(\mathbf{r})$, rel. units	$\nabla^2\rho(\mathbf{r})$, rel. units	E_b , kcal mol ⁻¹
	D—H	He···A	D···A					
O(5)—H(5A)···N(1) ⁱ	0.98	1.825	2.795(3)	171	16.2	0.050	0.067	-13.97
O(5)—H(5B)···O(4) ⁱⁱ	0.98	1.823	2.770(3)	173	23.3	0.042	0.086	-11.21
N(1)—H(1B)···O(3) ⁱⁱⁱ	0.87	2.301	2.995(4)	137	18.5	0.016	0.066	-3.63

* Symmetry codes: ⁱ 1 - x, 3/2 + y, 1 - z; ⁱⁱ x, 1 + y, z; ⁱⁱⁱ 1 + x, y, z.

Table 3. Integral characteristics of the main structural fragments in the structure of compound I*

Atom	Q_{theor} , \bar{e}	V_{theor} , Å ³	V_{VDP} , Å ³
K(1)	0.87	18.98	18.51
K(2)	0.85	20.28	18.45
H ₂ O	-0.28	26.61	29.15
L-Trp ₁	-0.62	249.65	250.10
L-Trp ₂	-0.82	254.39	253.87

a high accuracy (the error of volume estimation does not exceed 9% for the metal atoms and is lower than 1% for the anions). The volume of the anions is independent of the conformation (as shown previously for the Imatinib molecules [48]). The water molecule bears a partially negative charge (-0.28 \bar{e}), and the charge of the cations and anions ranges from +0.85 to +0.87 and from -0.82 to -0.62 \bar{e} , respectively. Note that the volumes of molecular domains of two anions with different conformations were close and the total energies of interactions (in which the anions participate) calculated as $0.5V(r)$ by the earlier proposed equation [49] were also close (-71.1 and -65.0 kcal

mol⁻¹). Almost 50% of this energy (47 and 43%) fall onto coordination bonds, 34 and 28% fall onto hydrogen bonds, and remained 19 and 29% correspond to hydrophobic interactions.

ACKNOWLEDGMENTS

XRD analysis was carried out using scientific equipment of the National Research Center Kurchatov Institute (Moscow, Russia). A.A. Korlyukov is grateful to the Samara Center for Theoretical Materials Science for access to computational resources and software.

FUNDING

XRD analysis and quantum chemical calculations were supported by the Russian Science Foundation, project no. 20-13-00241.

CONFLICT OF INTEREST

The authors declare that they have no conflicts of interest.

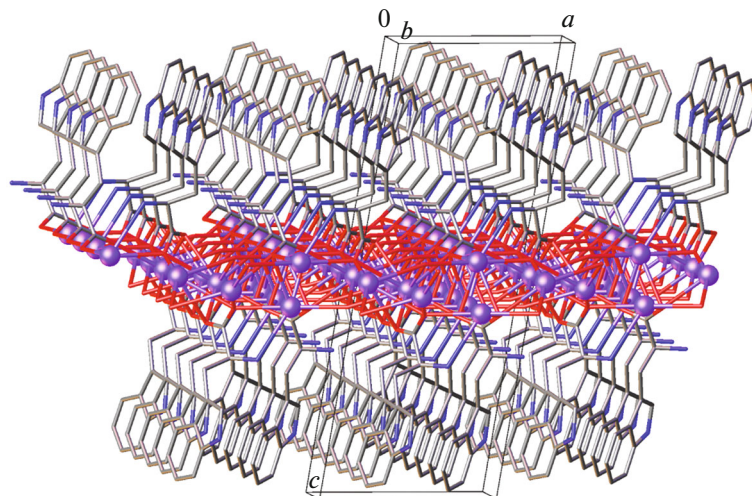


Fig. 5. Fragment of the layers in the structure of compound I. Potassium atoms are shown as spheres, and hydrogen atoms are omitted.

REFERENCES

1. Soldevila-Barreda, J.J. and Metzler-Nolte, N., *Chem. Rev.*, 2019, vol. 119, no. 2, p. 829.
<https://doi.org/10.1021/acs.chemrev.8b00493>
2. Saboury, A.A., *J. Iran. Chem. Soc.*, 2006, vol. 3, no. 1, p. 1.
<https://doi.org/10.1007/BF03245784>
3. Poursharifi, M., Włodarczyk, M.T., and Mieszkowska, A.J., *Inorganics*, 2019, vol. 7, no. 1, p. 2.
<https://doi.org/10.3390/inorganics7010002>
4. Palermo, G., Spinello, A., Saha, A., et al., *Expert Opin. Drug Discov.*, 2021, vol. 16, no. 5, p. 497.
<https://doi.org/10.1080/17460441.2021.1851188>
5. Vidossich, P. and Magistrato, A., *Biomolecules*, 2014, vol. 4, no. 3, p. 616.
<https://doi.org/10.3390/biom4030616>
6. Palermo, G., Magistrato, A., Riedel, T., et al., *ChemMedChem*, 2016, vol. 11, no. 12, p. 1199.
<https://doi.org/10.1002/cmdc.201500478>
7. Dey, D. and Basu, S., *J. Lumin.*, 2011, vol. 131, no. 4, p. 732.
<https://doi.org/10.1016/j.jlumin.2010.11.027>
8. Mosae Selvakumar, P., Suresh, E., and Subramanian, P.S., *Polyhedron*, 2009, vol. 28, no. 2, p. 245.
<https://doi.org/10.1016/j.poly.2008.10.072>
9. Maclare, J.K. and Janiak, C., *Inorg. Chim. Acta*, 2012, vol. 389, p. 183.
<https://doi.org/10.1016/j.ica.2012.03.010>
10. Wang, J., Xu, X.-Y., Ma, W.-X., et al., *Jiegou Huaxue*, 2008, vol. 27, p. 153.
11. Wang, J., Xu, X., Ma, W., et al., *Acta Crystallogr., Sect. E: Struct. Rep. Online*, 2007, vol. 63, no. 11, p. m2867.
<https://doi.org/10.1107/S1600536807053421>
12. Xie, Y., Wu, H.-H., Yong, G.-P., et al., *Acta Crystallogr., Sect. E: Struct. Rep. Online*, 2006, vol. 62, no. 9, p. m2089.
<https://doi.org/10.1107/S1600536806030364>
13. Mendiratta, S., Usman, M., Luo, T.-T., et al., *Cryst. Growth Des.*, 2014, vol. 14, no. 4, p. 1572.
<https://doi.org/10.1021/cg401472k>
14. Xiao, D.-R., Zhang, G.-J., Liu, J.-L., et al., *Dalton Trans.*, 2011, vol. 40, no. 21, p. 5680.
<https://doi.org/10.1039/C1DT0262A>
15. Mendiratta, S., Tseng, T.-W., Luo, T.-T., et al., *Cryst. Growth Des.*, 2018, vol. 18, no. 5, p. 2672.
<https://doi.org/10.1021/acs.cgd.8b00012>
16. Patra, A.K., Bhowmick, T., Ramakumar, S., et al., *Dalton Trans.*, 2008, no. 48, p. 6966.
<https://doi.org/10.1039/B802948B>
17. Şenel, P., İnci, D., Aydin, R., et al., *Appl. Organomet. Chem.*, 2019, vol. 33, no. 10, p. E5122.
<https://doi.org/10.1002/aoc.5122>
18. Kumita, H., Kato, T., Jitsukawa, K., et al., *Inorg. Chem.*, 2001, vol. 40, no. 16, p. 3936.
<https://doi.org/10.1021/ic000990p>
19. Lazarenko, V.A., Dorovatovskii, P.V., Zubavichus, Y.V., et al., *Crystals*, 2017, vol. 7, no. 11, p. 325.
<https://doi.org/10.3390/cryst7110325>
20. Svetogorov, R.D., Dorovatovskii, P.V., and Lazarenko, V.A., *Cryst. Res. Technol.*, 2020, vol. 55, no. 5, p. 1900184.
<https://doi.org/10.1002/crat.201900184>
21. Kabsch, W., *Acta Crystallogr., Sect. D: Biol. Crystallogr.*, 2010, vol. 66, no. 2, p. 125.
<https://doi.org/10.1107/S0907444909047337>
22. Evans, P., *Acta Crystallogr., Sect. D: Biol. Crystallogr.*, 2006, vol. 62, no. 1, p. 72.
<https://doi.org/10.1107/S0907444905036693>
23. Sheldrick, G.M., *Acta Crystallogr., Sect. A: Cryst. Adv.*, 2015, vol. 71, no. 1, p. 3.
<https://doi.org/10.1107/S2053273314026370>
24. Sheldrick, G.M., *Acta Crystallogr., Sect. C: Struct. Chem.*, 2015, vol. 71, no. 1, p. 3.
<https://doi.org/10.1107/S2053229614024218>
25. Dolomanov, O.V., Bourhis, L.J., Gildea, R.J., et al., *J. Appl. Crystallogr.*, 2009, vol. 42, no. 2, p. 339.
<https://doi.org/10.1107/S0021889808042726>
26. Peresypkina, E.V. and Blatov, V.A., *Acta Crystallogr., Sect. B: Struct. Sci.*, 2000, vol. 56, no. 3, p. 501.
<https://doi.org/10.1107/S0108768199016675>
27. Peresypkina, E.V. and Blatov, V.A., *Acta Crystallogr., Sect. B: Struct. Sci.*, 2000, vol. 56, no. 6, p. 1035.
<https://doi.org/10.1107/S0108768100011824>
28. Blatov, V.A., Shevchenko, A.P., and Proserpio, D.M., *Cryst. Growth Des.*, 2014, vol. 14, no. 7, p. 3576.
<https://doi.org/10.1021/cg500498k>
29. Kresse, G. and Hafner, J., *Phys. Rev. B*, 1993, vol. 47, no. 1, p. 558.
<https://doi.org/10.1103/PhysRevB.47.558>
30. Kresse, G. and Hafner, J., *Phys. Rev. B*, 1994, vol. 49, no. 20, p. 14251.
<https://doi.org/10.1103/PhysRevB.49.14251>
31. Kresse, G. and Furthmüller, J., *Phys. Rev. B*, 1996, vol. 54, no. 16, p. 11169.
<https://doi.org/10.1103/PhysRevB.54.11169>
32. Kresse, G. and Furthmüller, J., *Comput. Mater. Sci.*, 1996, vol. 6, no. 1, p. 15.
[https://doi.org/10.1016/0927-0256\(96\)00008-0](https://doi.org/10.1016/0927-0256(96)00008-0)
33. Kresse, G. and Joubert, D., *Phys. Rev. B*, 1999, vol. 59, no. 3, p. 1758.
<https://doi.org/10.1103/PhysRevB.59.1758>
34. Gonze, X., Beuken, J.-M., Caracas, R., et al., *Comput. Mater. Sci.*, 2002, vol. 25, no. 3, p. 478.
[https://doi.org/10.1016/S0927-0256\(02\)00325-7](https://doi.org/10.1016/S0927-0256(02)00325-7)
35. Tang, W., Sanville, E., and Henkelman, G., *J. Phys.: Condens. Matter.*, 2009, vol. 21, no. 8, p. 084204.
<https://doi.org/10.1088/0953-8984/21/8/084204>
36. Bader, R.F.W., *Atoms in Molecules: A Quantum Theory*, Clarendon, 1994, p. 438.
37. Bader, R.F.W., *Acc. Chem. Res.*, 1985, vol. 18, no. 1, p. 9.
<https://doi.org/10.1021/ar00109a003>
38. Korlyukov, A.A., Khrustalev, V.N., Vologzhanina, A.V., et al., *Acta Crystallogr. Sect. B: Struct. Sci.*, 2011, vol. 67, no. 4, p. 315.
<https://doi.org/10.1107/S0108768111022695>
39. Vologzhanina, A.V., Savchenkov, A.V., Dmitrienko, A.O., et al., *J. Phys. Chem. A*, 2014, vol. 118, no. 41, p. 9745.
<https://doi.org/10.1021/jp507386j>

40. Vologzhanina, A.V. and Lyssenko, K.A., *Russ. Chem. Bull.*, 2013, vol. 62, no. 8, p. 1786.
<https://doi.org/10.1007/s11172-013-0257-0>
41. Serezhkin, V.N., Serezhkina, L.B., and Vologzhanina, A.V., *Acta Crystallogr. Sect. B: Struct. Sci.*, 2012, vol. 68, no. 3, p. 305.
<https://doi.org/10.1107/S0108768112014711>
42. Serezhkin, V.N. and Savchenkov, A.V., *Cryst. Growth Des.*, 2015, vol. 15, no. 6, p. 2878.
<https://doi.org/10.1021/acs.cgd.5b00326>
43. Serezhkin, V.N. and Savchenkov, A.V., *Cryst. Growth Des.*, 2020, vol. 20, no. 3, p. 1997.
<https://doi.org/10.1021/acs.cgd.9b01645>
44. Serezhkin, V.N. and Savchenkov, A.V., *CrystEngComm*, 2021, vol. 23, no. 3, p. 562.
<https://doi.org/10.1039/D0CE01535K>
45. Vologzhanina, A.V., *Crystals*, 2019, vol. 9, no. 9, p. 478.
<https://doi.org/10.3390/cryst9090478>
46. Zorina-Tikhonova, E.N., Chistyakov, A.S., Kis-kin, M.A., et al., *Russ. J. Coord. Chem.*, 2021, vol. 47, no. 6, p. 409.
<https://doi.org/10.1134/S1070328421060099>
47. Karnoukhova, V.A., Baranov, V.V., Vologzhanina, A.V., et al., *CrystEngComm*, 2021, vol. 23, no. 24, p. 4312.
<https://doi.org/10.1039/D1CE00434D>
48. Vologzhanina, A.V., Ushakov, I.E., and Korlyukov, A.A., *Int. J. Mol. Sci.*, 2020, vol. 21, no. 23, p. 8970.
<https://doi.org/10.3390/ijms21238970>
49. Espinosa, E., Molins, E., and Lecomte, C., *Chem. Phys. Lett.*, 1998, vol. 285, no. 3, p. 170.
[https://doi.org/10.1016/S0009-2614\(98\)00036-0](https://doi.org/10.1016/S0009-2614(98)00036-0)

Translated by E. Yablonskaya